# CHAPTER-9

# TECTONO-METAMORPHIC EVOLUTION

This chapter discusses the tectono-metamorphic evolution considering petrographic evidence, geochronological evidence, *P-T-t* path, and geodynamic conditions. The metamorphic evolution of the study area around Mauranipur and Babina reveals a wide variety of rocks, which are affected by three stages of metamorphism ($M_1$ to $M_3$). Mauranipur and Babina areas have well-preserved Archean age rocks, which leads to the Bundelkhand Craton (BuC) being part of the Ur and Kenorland supercontinent.

## 9.1 Metamorphic condition

Different methodologies are applied to extract the rock history, which provides crucial datasets constraining the evolution of BuC. The evolutionary accounts of granulite are preserved in different mineral assemblages and associations in different rock types, fabrics and textural relations. In addition to the significance of the physical mineral textures, other imperative components such as major, trace and rare earth elements and their isotopic composition provide crucial information about the rock's genesis and evolution. The objective of estimating *P–T* and calculating mineral equilibria is to decipher relevant information on granulitic rocks, which provides reliable information relating to their burial and exposure on the surface through geological time.

The Mauranipur and Babina areas have been studied based on tools such as petrography, mineralogy, phase petrology, geothermobarometry, phase equilibria modelling, geochronology and geochemistry; based on this, the construction of the *P–T* path was done to divulge its metamorphic evolution.

### 9.1.1 Petrographic evidences

Metamorphic petrology has been employed to decoding the mineral assemblage and microstructural record of burial/exhumation and heating/cooling imprinted on pre-existing sedimentary, igneous and metamorphic rocks by processes such as subduction, accretion and collisional orogenesis. Petrologists address various activities, from the *P-T-t* evolution of rock in space and time. The quantitative *P–T–t* paths provide information to parameterize subduction zone processes and collisional orogenesis. Incorporating this *P-T-t* information, it delivers information about the geodynamic and tectono-metamorphic evolution and reveals the history of lithosphere evolution.

#### 9.1.1.a Pelitic granulites

**Prograde assemblage**

During the near-peak stage, the garnet grew continuously with the consumption of biotite and plagioclase according to the following biotite-melting dehydration reaction (Vielzeuf and Montel, 1994) (Fig. 4.2b):

Bt + Sil + Qz → Grt + K-fs + Melt

**Peak assemblage**

As the pressure begins to increase, coarse-grained orthopyroxene is introduced, and in places, small garnet relicts are present in adjacent to altered orthopyroxene (Fig.4.2c,d), reflecting the following reactions (Vielzeuf and Montel, 1994):

Bt + Pl + Qz → Opx + Grt + Melt

**Post-peak assemblage**

As the pressure continuously descended, matrix cordierite is formed in association with matrix biotite, quartz, and plagioclase (Fig. 4.2e). The probable reaction texture has been identified, as cordierite grains are present in the vicinity of garnet grains (Fig. 4.2f).

Grt + Bt + Qz → Crd + Melt

### 9.1.1.b Garnet-biotite gneisses

**Prograde assemblage**

During prograde metamorphism, biotite reacts with quartz to form garnet. It contains an inclusion of biotite along with plagioclase and quartz at various places (Figs.4.6a,b), suggesting the following reaction:

Bt + Pl + Qz → Grt + K-fs + Melt

**Post-peak assemblage**

In some of the thin sections, biotite and quartz border the porphyroblasts of garnet, which provides evidence for late hydration during cooling (Fig.4.6c,d) as the pressure continuously decreases, indicating the following reaction:

Grt + Pl + Melt → Bt + Qz

### 10.1.1.c Amphibolites

**Pre-peak assemblage**

The pre-peak metamorphic assemblage has been recognized as Grt-Amp-Chl-Bt-Pl-Ilm-Qz, which contains amphibole, chlorite, biotite, plagioclase, and ilmenite as inclusions inside garnet porphyroblast. This phase has preserved mineral inclusions that are consumed during prograde metamorphism (Figs.4.9 b&c). These textural features suggest a pre-peak prograde metamorphic condition.

**Peak assemblage**

The formation of medium-grained clinopyroxene is observed in association with porphyroblastic garnet and amphibole (Fig.4.9d). The Grt-Amp-Cpx-Bt-Pl-Ilm-Qz assemblages in the garnet-bearing amphibolite characterize the peak metamorphic assemblage. It infers that the peak metamorphic assemblage is formed by following reactions

Amp + Qz → Cpx + Grt + Melt

**Post-peak assemblage**

The post-peak metamorphic assemblage is defined by Amp-Bt-Pl-Ilm-Qz. The post-peak condition in this rock is indicated by a few reaction textures, where amphibole is formed by the breakdown of garnet and clinopyroxene. Here amphibole is present as a majority in the matrix phases (Fig.4.9f). The following reactions are inferred

Cpx + Melt → Amp + Bt + Qz

Grt + Bt + Melt → Amp + Qz + Melt

### 9.1.2 P-T-t Path

Three types of thermodynamics methods were used to compute *P–T* conditions, i.e., conventional (mono-equilibrium) geothermobarometry, multi-equilibrium geothermometry, and forward modelling. These methods yielded more or less same results for granulites, Garnet-biotite gneisses and amphibolites of the BuC. *P-T-t* paths represent a rock or a terrain through *P–T* space with time. It is the sequence of *P–T* conditions experienced by a rock unit during regional metamorphism. The *P–T* path can be grouped into two types: clockwise and anti-clockwise. Peak temperatures follow the peak pressures in the clockwise *P–T* path, and peak pressures succeed the peak temperature in the anti-clockwise path. The proper evolution of *P–T* paths is essential to formulate the tectonic models for the evolution of granulite terrains. *P–T* paths can be inferred using estimates of pressure and temperature from the minerals' paragenetic sequence.

The data provided by geothermobarometry for the metamorphic rocks of the study area suggest that these high-grade rocks have witnessed and undergone various geodynamic processes through a various degree of change in pressure and temperature along with the Earth's history, this metamorphic evolution of granulites concerning time represents a *P-T-t* path of the rock. The determination of the pressure-temperature path of metamorphic rocks is one of the most critical aspects in understanding the rocks' evolution since it can reveal many constraints such as the heat and pressure achieved during peak metamorphism, local structural setting and tectonic process. Many workers have derived the *P–T* path in investigating the evolution of Orogenic belts through time (Vance et al., 1998; Marschall et al., 2003). Qualitative and quantitative methods can estimate the pressure and temperature experienced by metamorphic rocks and subsequent cooling or decompression during upliftment.

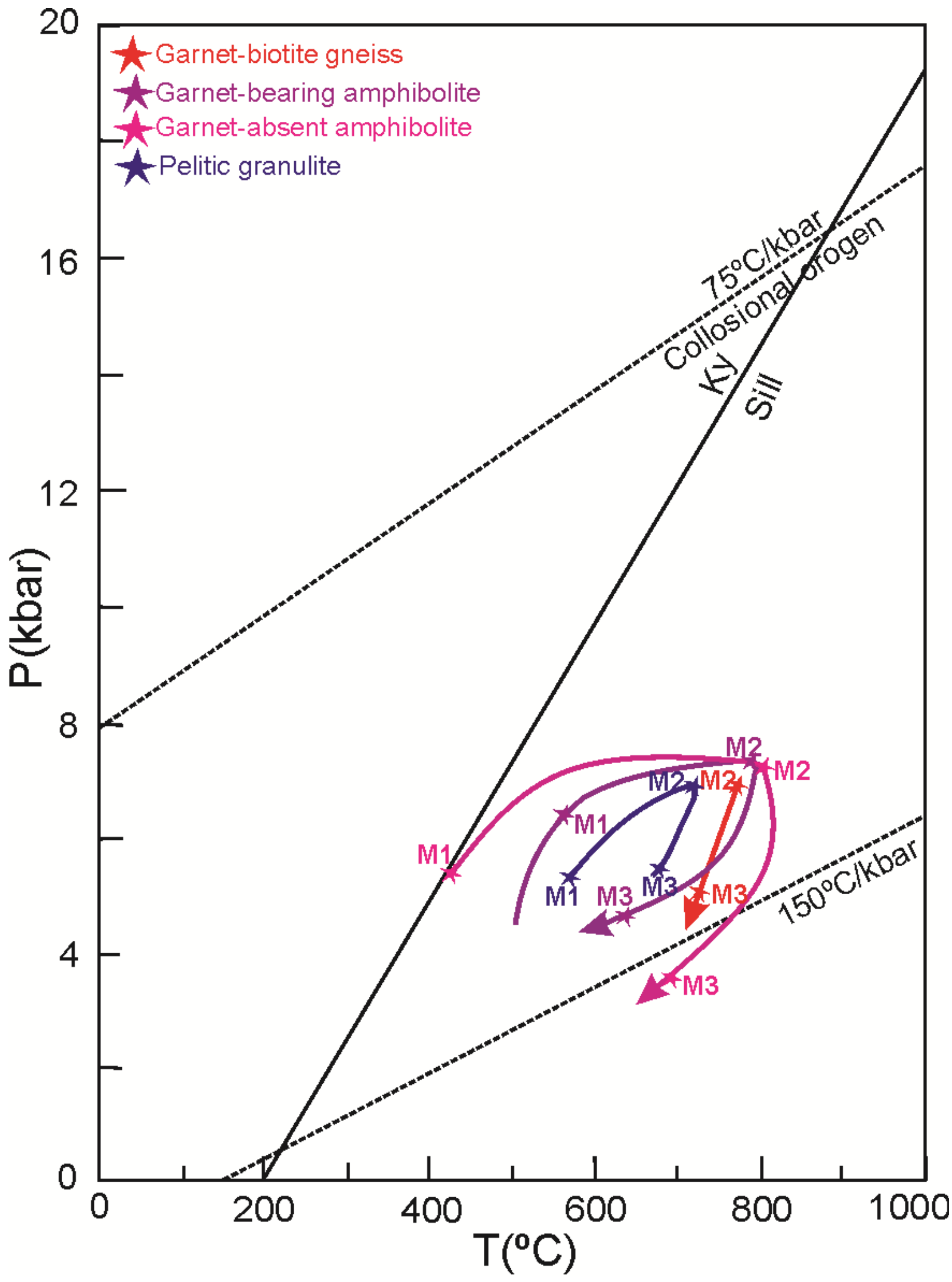


**Figure 9.1** P-T-t path represents the metamorphic stages of all the three studied rocks.

The *P–T* path has been constrained for BuC, using three different rock types: pelitic granulites, garnet-biotite gneisses and amphibolites. A combination of micro-textures, mineral prograde and retrograde reactions, and the *P–T* estimates derived from mineral chemistry data of coexisting mineral pairs have been utilized to evaluate the different metamorphism grades *P-T-t* paths. Based on geological, petrographic and micro-textural studies, it is inferred that the various rock types in the study area have undergone a granulite facies metamorphism and suggest a distinct near Isothermal Decompression (ITD) path. A *P-T-t* path has been constructed for all three studied rocks which show the different metamorphic stages (Fig.9.1).

**9.1.2.a Pelitic granulites**

The clockwise *P-T-t* path has been obtained from orthopyroxene-bearing pelitic granulites by thermodynamic calculation and pseudosection modelling. The pre-peak metamorphic stage was recorded between 4.00–5.12 kbar and 560–600°C. This rock undergoes further burial depth, and with a significant change in temperature conditions, this situation indicates an increase in pressure; hence it demarcated the peak metamorphic stage. The *P–T* conditions of this stage reached a high-pressure condition with a range of 6.40–6.62 kbar and 700–730°C, following a nearly isothermal decompression (ISD) path to achieve the post-peak stage. The post-peak stage was documented by the appearance of Crd, and Grt, and *P–T* conditions were reached at 4.20–4.40 kbar and 670–692°C. The geodynamic significance of the peak (high-pressure) metamorphism from the Mauranipur region of the CBGB suggests subduction and exhumation in a single cycle as a complete clockwise *P-T-t* path. Various P-T-t paths have been proposed from different localities within the BuC, most of which represent the clockwise paths (Fig.9.1).

### 9.1.2.b Garnet-biotite gneisses

The metamorphic assemblages and textural relationship have been described with special emphasis for garnetiferous Mauranipur garnet-biotite gneisses. The garnet-biotite gneisses are characterized by the mineral assemblage garnet + biotite + plagioclase + k-feldspar + ilmenite + quartz + melt. *P–T* pseudosection modelling shows mineral assemblage Grt-Bt-Pl-Kfs-melt-Ilm-Qz to be stable at the *P–T* range of 6.35–6.75 kbar and 755–780ºC. Bulk rock composition modelling provides significant knowledge about mineral nucleation, development, and ingestion in multivariate mineral assemblages, as well as regarding alleged microstructures with prograde metamorphism until achieving the peak condition; it can be shown by comparative changes in the expected mineral abundances (in mol% ).

*P–T* estimation and pseudosection modelling in the NCKFMASHT system was shown the garnet-biotite gneisses experienced metamorphism of pentavariant stability field (Grt, pl, k-fs, bt, ilm, qz, melt) stable at the *P–T* range of 6.35–6.75 kbar and 755–780ºC. We have also observed similar mineral assemblages under lower pressure and temperature conditions. The melt phase does not exist here, whereas $H_2O$ is available as a component. Therefore, we would like to say that this stable phase may evolve during the retrograde metamorphic condition. Their *P–T* condition is comparatively low, which is between 4.80–5.28 kbar and 718–735ºC. The geochemical interpretation provides significant evidence that the garnet-biotite gneisses were generated in a subduction zone tectonic setting, and the protoliths of garnet-biotite gneisses were further metamorphosed by the continent-continent collision (Fig.9.1).

### 9.1.2.b Amphibolites

Since the Archean age, several magmatic emplacements have been observed in the BuC, and it has also preserved three dominant stages of metamorphism at ~3200 Ma, ~2500 Ma, and ~2100 Ma. We have also established evidence for three metamorphic stages from garnet-bearing and garnet-absent amphibolites from the Mauranipur and Babina regions using mineral assemblages, textural correlations, and *P–T* pseudosections. The clockwise *P–T* path is constrained by the *P–T* pseudosection of garnet-bearing amphibolite (B-6) from the Babina region (Fig. 9.1). This *P–T* path generates three prominent metamorphic assemblages, as well as a previously developed meta-stable mineral assemblage. The meta-stable mineral assemblage Amp-Chl-Bt-Pl-Qz-Ilm appears at the 4.35–4.1 kbar/515–475ºC *P–T* condition, suggesting a primitive mineral assemblage. Garnet was not visible at this temperature, but as it rises, it formed a unique mineral assemblage Grt-Amp-Chl-Bt-Pl-Qz-Ilm, which is stable in a narrow region with a *P–T* range of 6.5–6.25 kbar/590–580ºC. This assemblage forms under amphibolite facies conditions during the pre-peak metamorphic stage. Later, the Babina region experienced the burial tectonism, which was characterized by a continuous increase in pressure and temperature, and the amphibolites underwent peak metamorphism until the granulite facies metamorphism, characterized by the mineral paragenesis Grt-Amp-Cpx-Bt-Pl-Qz-Ilm-$H_2O$, and this field is stable at 7.4–6.8 kbar/805–760ºC. The mineral assemblage of the post-peak metamorphic stage Amp-Bt-Pl-Qz-Ilm, is stable at a *P–T* range of 4.75–4.45 kbar/615–585ºC, which acquires a Cpx and Grt free field. This post-peak stage occurred after the peak stage as a result of a decompression process that resulted in a decrease in pressure conditions, also known as isothermal cooling, implying that this stage may have developed as a result of decompression and subsequent exhumation of amphibolites on the surface.

### 9.2 Geodynamic conditions

The lithospheric evolution and Earth's thermal evolution is a response to geodynamics. There are significant variations recorded in the geological and tectonic style between the Archean and post-Archean crusts. Tonalite–trondhjemite–granodiorite (TTG) and grey gneisses suites are dominated in the Archean terrains, with volcano-sedimentary greenstone belts forming a minor component (Goodwin et al., 1996). However, the Earth's thermal evolution is poorly constrained (Korenaga et al., 2006, 2008, 2011,, 2013; Hunen et al., 2012); it is likely that before Archean (3.0 Ga), heating was mainly due to the decay of radioactive substances that would lead to surface heat loss, whereas post-Archean (ca 2.5 Ga) period was dominated by secular cooling (Brown et al., 2003).

### 9.2.1 Proposed geodynamic models

The geodynamic context of the Bundelkhand rocks, which span the Paleo-Mesoarchean, Neoarchean, and Paleoproterozoic periods, have been subjected to severe magmatism and metamorphism, and has been a long-standing topic in Indian geology. Due to a lack of comprehensive data involving mineral chemistry, isotope and bulk chemistry, and geochronological inputs, it remains strongly limited. Various authors have given the geodynamic model of the evolution of BuC, such as Chauhan et al., 2018 (Fig. 9.2), Slabunov and Singh (2019) (Fig. 9.3), Singh et al., 2019 (Fig. 9.4), Hildori et al., 2021 Singh et al., 2019, 2021 etc. The authors and coworkers identified the Central and Southern Bundelkhand greenstone complexes in the craton (Singh and Slabunov, 2016, 2019; Singh et al., 2021). The Babina and Mauranipur Greenstone Belts (GBs) form the Central Bundelkhand Greenstone Belt (CBGB), which has an E-W linear trend. An early (Mesoarchean) assemblage of basic-ultrabasic, felsic volcanic (2.8 Ga), and BIF rocks; and a late (Neoarchean – ca. 2.54 Ga) assemblage of felsic volcanic rocks make up this complex. A polymetamorphic evolution pattern can be seen in the CBGB. Paleoarchean amphibolite/granulite-facies and Mesoarchean eclogite-facies metamorphic events have been discovered (Saha et al., 2011; Nasipuri et al., 2019), although Neoarchean amphibolite-facies metamorphism (at least 586–679 °C and 6.7–7.2 kbar) is more common. These metamorphic stages in the craton may be linked to metasomatic occurrences. The most recent metamorphism in the cratonic rocks occurred locally under prehnite-pumpellyite facies conditions and was likely triggered by Paleoproterozoic (ca 1.9–1.8 Ga) rifting (Slabunov and Singh, 2019).

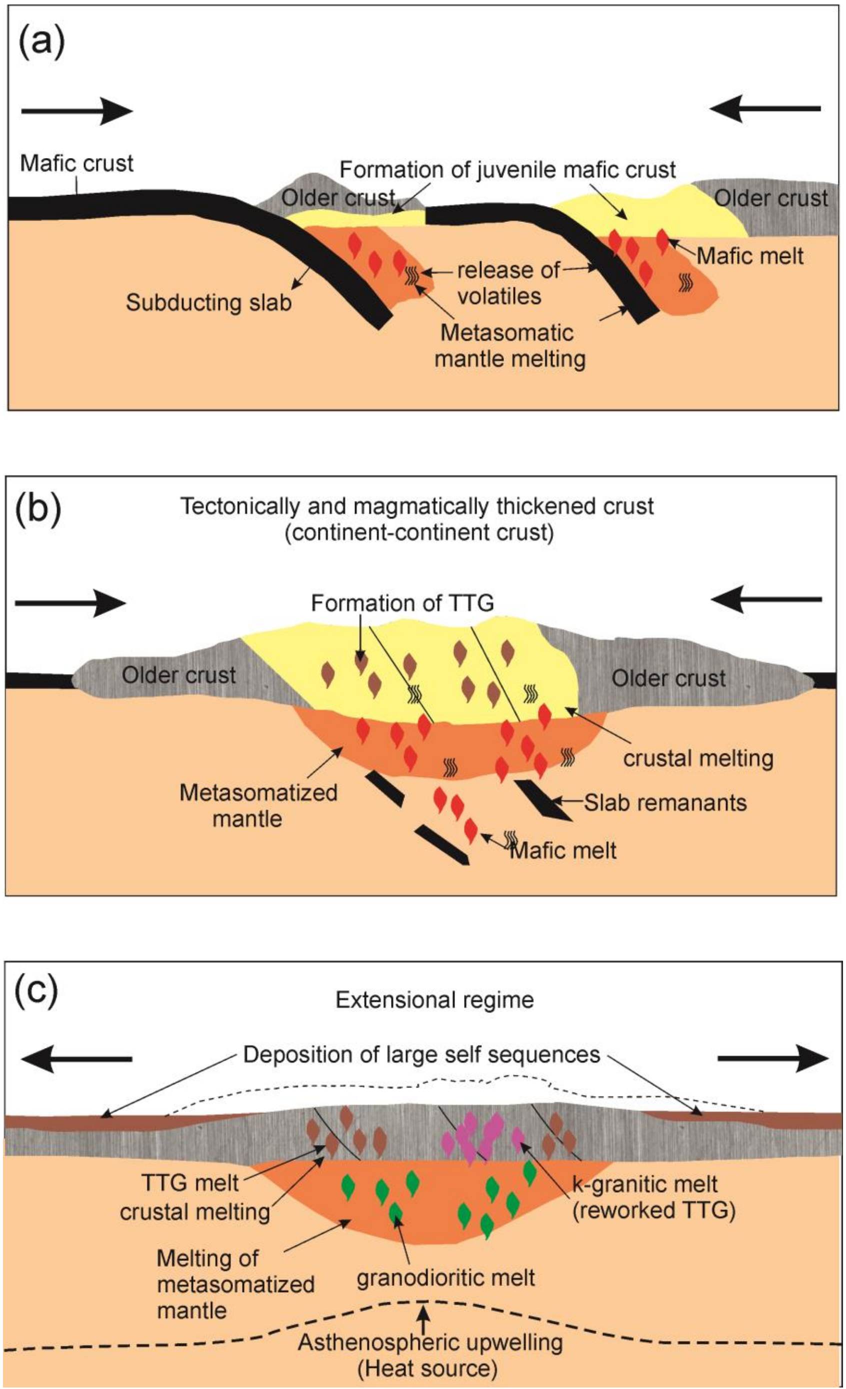


**Figure 9.2** Model proposed by the Chauhan et al., 2018, illustrating the proposed geodynamic setting for the evolution of TTG and associated K-granites in the Bundelkhand craton. Stage (a): During this stage, subduction takes place with possible episodic breakoff of the slab, Stage (b): The first stage ultimately leads to closure of an ocean basin and wielding of two proto-continental blocks (continental collision). Stage (c): In the late- to post-collisional stage owing to thermal relaxation and extension, melting of the previously generated TTG crust ensues resulting in generation of the K-granites.

Chauhan et al., 2018 proposed a geodynamic model (Fig. 9.2) based on the geochemical features of the TTGs and K-rich granites. According to their study, two types of terrane compose the Precambrian basement of the Bundelkhand craton. The first is a high-grade metamorphic terrane with tonalite, trondhjemite, granodiorites, and supracrustal rocks (ultramafic to mafic igneous and sedimentary rocks with BIF), and the second is a granitic terrane with no metamorphism. All of these rocks date from 3.5 to 2.6 Ga and have undergone granulite facies metamorphism between 2.7 and 2.4 Ga. An intensive tectonothermal event in the late Neoarchean in BuC is indicated by the plutonic magmatism (2.6–2.5Ga) and the high-grade metamorphism of (2.7–2.4 Ga) as reported by Saha et al., (2011). The Paleo-Mesoarchean TTG granitoids were formed by partial melting of Eoarchean enriched mafic crustal sources at various depths, demonstrating crustal thickening caused by micro-continental collision. With their intrusive contact with TTG gneisses and younger age, the K-rich granites reflect the last episode of Archaean magmatism in BuC. K-rich granites were produced by the remelting of Paleo-Mesoarchean TTGs or mafic crust in an extensional/non-compressional regime associated with a post-orogenic or post-collisional stage. The composition of the melt produced by melting of the Paleo-Mesoarchean mafic crust is again modified due to the continuous uprising of the upwelling mantle. As a result, hornblende-bearing granites, biotite-bearing granites and leucogranites were produced. The extensional event that produced enormous potassic granite plutons can be linked to the dyke swarms, quartz reefs, and marginal basins of Gwalior and Bijawar in this region.

Slabunov and Singh (2019) proposed a geodynamic model (Fig. 9.3) of the BuC based on the isotopic and geochemical analysis of the volcanic and metasomatic rocks of the CBGB. According to their study, the BuC has evolved through two subduction–accretion events, the Meso–Neoarchaean (2.81–2.7 Ga) and Neoarchaean (2.56–2.53 Ga).

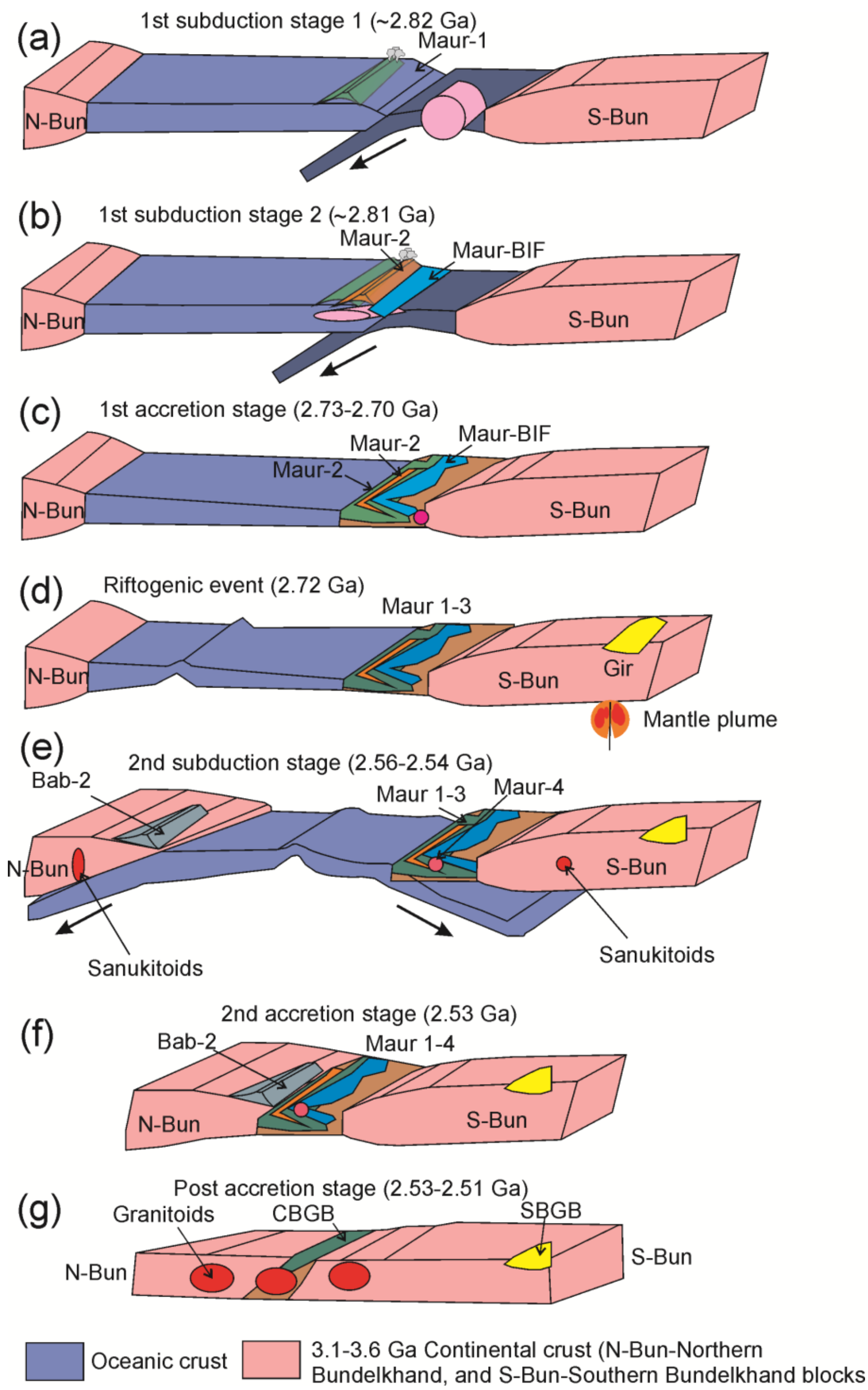


**Figure 9.3** Geodynamic model of the crustal evolution of the Bundelkhand Craton proposed by the Slabnov et al., 2019, during 2.82–2.5 Ga, Maur-1-4: assemblage-1-4 of CBGC in Mauranipur belt and Bab2: formation-2 of CBGC in Babina belt.

Subduction processes in the oceanic (initial) island-arc system establish the association of felsic volcanites (2810±13 Ma) and basic-ultramafic rocks (Malviya et al. 2006). Volcanism in the island arc is followed by dacitic–rhyolitic volcanism. The subductional character of the BuC is highly supported by the same age of the eclogite-facies metamorphic event (2.780±60 Ga) (Saha et al. 2011), in the Babina belt and island-arc dacitic–rhyolitic volcanism (2.810±13 Ga). BIFs are deposited in the second stage from either a fore-arc or back-arc basin, with terrigenous materials coming from an accretionary wedge (Mauranipur BIFs) or a volcanic arc (Babina BIFs) (Singh and Slabunov 2015a). The arc complex accreted to the southern continental block around 2.7 Ga, evidenced by the thrust faults seen in the Mauranipur belt. At 2.56–2.54 Ga, a spreading zone appears in the subduction which separated the northern and southern blocks; however, the rate of its opening was slower than the rate of subduction at the periphery. Subduction occurred in an active continental margin regime near the northern block's southern margin, as evidenced by the Neoarchaean (2.542 Ga; Singh and Slabunov 2015a) felsic volcanites of the Babina belt and a sanukitoid massif of similar age (2.560–2.559 Ga; Joshi et al. 2017). This stage is defined by the Neoarchaean (2.557 Ga; Singh and Slabunov 2019) dacites of the Mauranipur belt and a sanukitoid massif on the northern flank of the southern continental block (Joshi et al. 2017). After the youngest (2.542 Ga) volcanism but before the creation of the earliest post-kinematic granites of 2.531 Ga, the ocean closed and the subsequent accretionary stage in the evolution of the greenstone complex occurred around 2.53 Ga. (Verma et al. 2016). The Mesoarchaean and Neoarchaean elements were united at this point to produce a single greenstone complex. Post-accretionary activities in the crust are linked to the melting of substantial amounts of granitoids between 2.53 and 2.51 Ga. Around 2.5 Ga, the craton was stabilized.

Singh et al. 2019 have proposed a geodynamic model (Fig. 9.4) based on In-situ U-Pb ages, whole rock analysis and Sm-Nd isotopic values of late Archean Sanukoitoids and high-K anatectic granites of the BuC to explain the formation and evolution of late-Archean rocks in the BuC. The oceanic slab was subducted at around 2.7 Ga, and the partial melting of hydrated garnetiferous mafic rocks mixed with the underlying mantle to generate TTG (granodioritic) melts (Fig. 9.4a) (Verma et al., 2016). The younger felsic volcanic present in the CBGB are generated through the upwelling of the lithospheric mantle by the subduction of the mid-oceanic ridge (Fig. 9.4b). Due to progressive cooling around 2.5 Ga, mantle peridotite heavily contaminated the slab melts, resulting in the formation of low-Ti sanukitoids (Fig. 9.4c). As a result, sanukitoid suites and high-K anatectic granites are likely to have played a crucial part in the overall crustal stabilization of BuC. Finally, at about 2.5 Ga, when the Earth's heat production was very low for slab melting, except in relatively occasional geodynamic settings, a critical transition occurred, and the craton was stabilized.

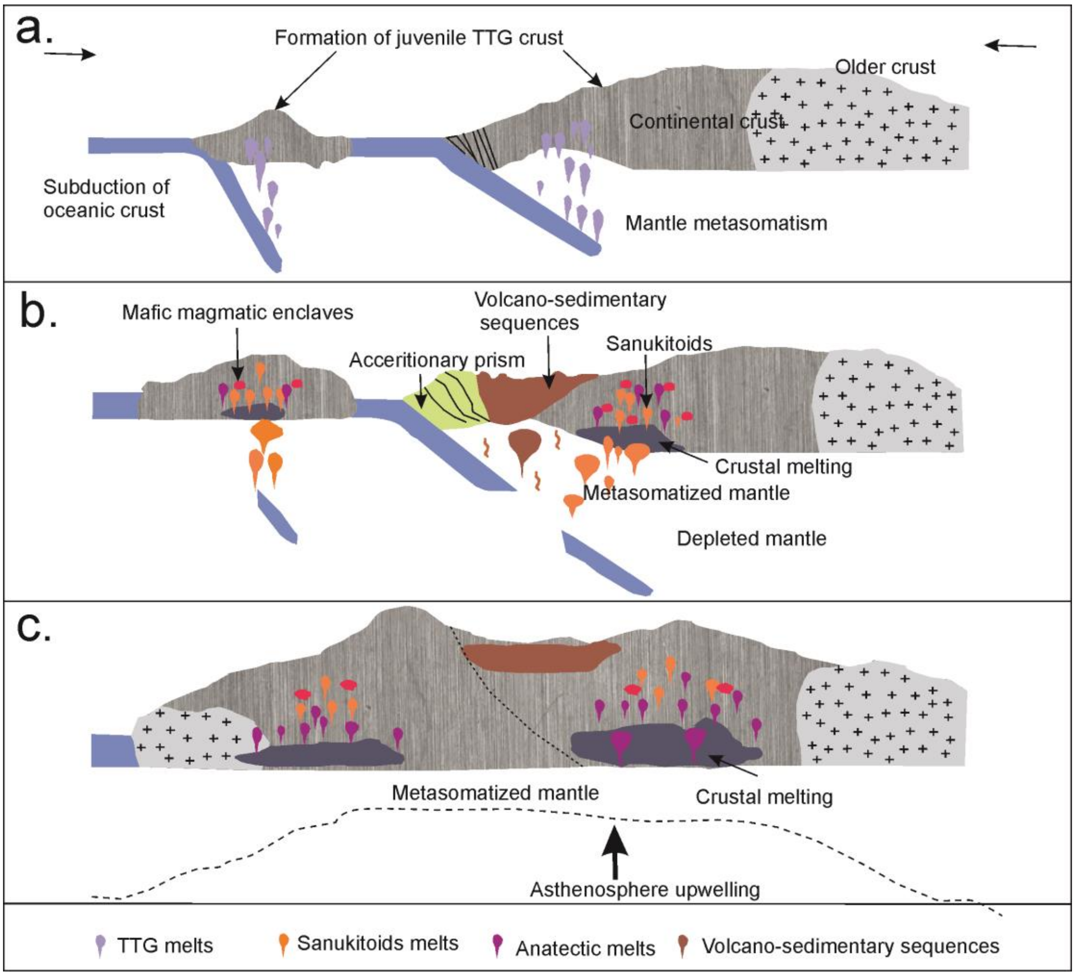


**Figure 9.4** Schematic, conceptual cartoon illustrating the proposed geodynamic model for evolution of the Bundelkhand Craton: (a) Geodynamic model showing the melting of subducted slab and mantle for the formation of TTGs at ~2.7 Ga, (b) followed by a shift from slab melting to direct mantle melting as a consequence of slabs break off into asthenosphere leading to mantle upwelling which caused origin of sanukitoids and also happened felsic volcanism at ~2.58 Ga, (c) finally, at ~2.5 Ga collision was happened and it provided heat flux to generate voluminous anatectic melts (anatexis processes).

### 9.2.2 Present study

The present study proposes a geodynamic model of the BuC based on the *P–T* conditions, geochemical analysis and geochronology of the pelitic granulites, garnet-biotite gneisses and amphibolites from the BuC.

The amphibolites have significant similarities in petrographic reaction texture, mineral chemistry, geochemical composition, geothermobarometry, and bulk composition modelling and can be interpreted as being generated by the same magma but solidifying at different depths. The pseudosection has provided a *P–T* condition between meta-stable and pre-peak metamorphism in the transition from greenschist to amphibolite facies. However, the appearance of garnet with clinopyroxene and associated mineral paragenesis indicates sufficient pressure and temperature to equilibrate the granulite facies. Both amphibolites register a clockwise path with peak metamorphism, followed by prograde and then retrograde metamorphism, showing three distinct compositions in the three stages of amphiboles. The rock classification diagram indicates that the rocks are basaltic to basaltic-andesite in composition and that they descended from the same protolith. The diverse mineralogical characteristics are due to distinct metamorphic grades; the $Zr/TiO_2$ vs Nb/Y diagram shows that there was only minor contamination during metamorphism. The petrographical reaction texture, phase equilibria modelling, and geochemical signatures of garnet-bearing and garnet-absent amphibolites from the Mauranipur and Babina regions have supported the geodynamics model for amphibolite evolution (Fig. 9.5). The central part of the BuC includes enclaves of mafic-ultramafic, amphibolites, schists, BIF and metasedimentary rocks within the basement of TTGs and granitoids. The protoliths of both amphibolites from the Mauranipur and Babina regions were formed by subduction-related tectonic settings and further affected by various thermal and collisional events.

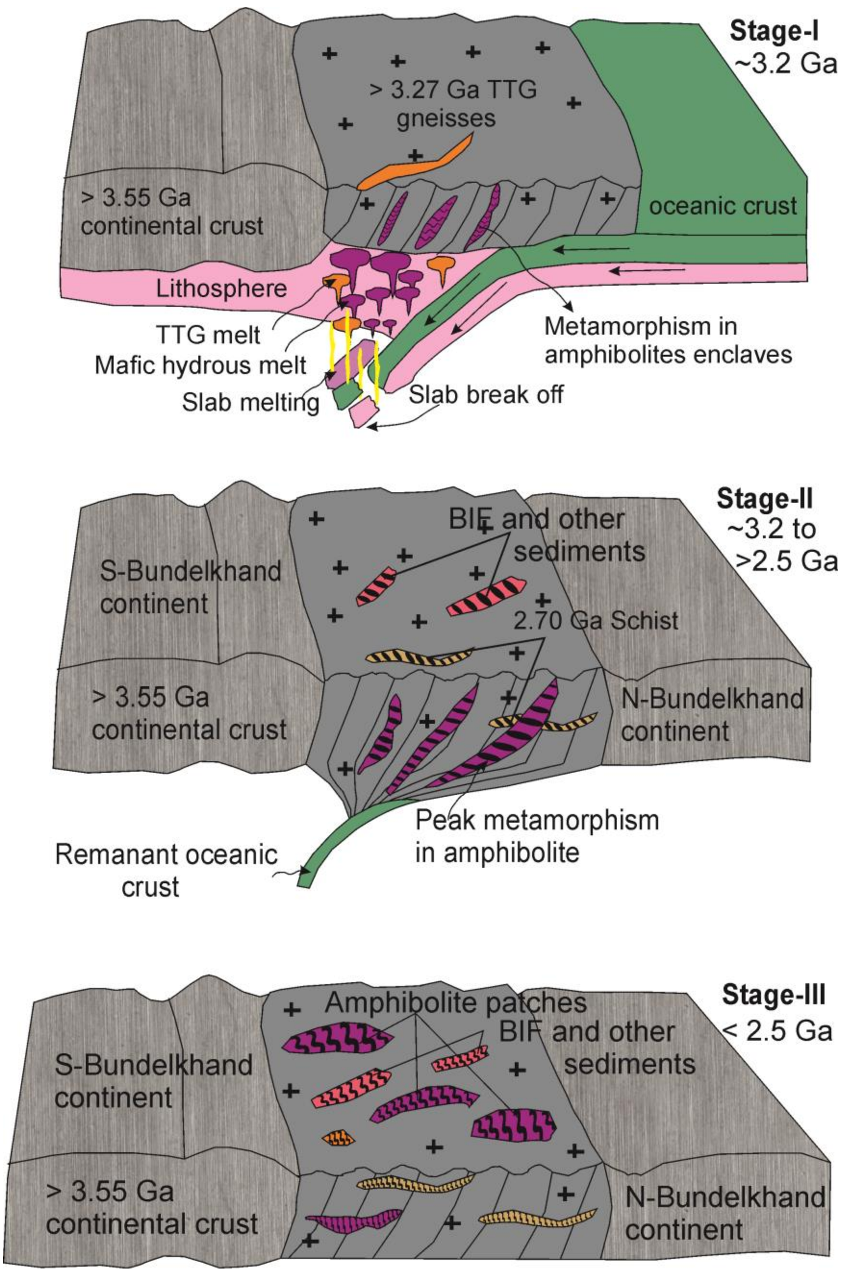


**Figure 9.5** Cartoon diagram showing the three stages of the tectono-metamorphic evolution model of the BuC. (Stage-I): it was demarcated between ~3.5 to 3.2 Ga, here subduction-related setting observed and entrapment of mafic magma in the basement of TTGs occurred (Sarkar et al. 1996; Singh et al. 2019). At ~3.2 Ga first metamorphism was recorded, which was experienced by amphibolites (Malviya et al. 2006; Mondal et al. 2002), TTGs (Kaur et al. 2016), and BIFs (Raza et al. 2021). (Stage-II): Further collision tectonism was demarcated in ~2.5 Ga, which leads to peak metamorphic condition in the BuC (Mondal et al. 2002), recorded by various rock types such as corundum-bearing schist (Saha et al. 2011), BIFs (Raza et al. 2021), metabasalt or amphibolites (Slabunov& Singh, 2018). (Stage-III): It is the third stage of metamorphism, which occurs after the stabilization of the BuC, and this stage is characterized by retrograde metamorphism. Few retrograde metamorphismis reported in some metamorphic rock types such as corundum-bearing schist (Saha et al. 2011), monazite overgrowth in BIFs (Raza et al. 2021), also some mafic dykes were intruded in ~2.1 to 2.0 Ga (Rao et al. 2005; Pradhan et al. 2012).

The studied amphibolites exist as enclaves and intrusive bodies and have undergone various metamorphic events, which are schematically represented as a plausible geodynamic model for three different stages.

### 9.3 Global correlation of BuC with the Ur and Kenorland supercontinent

Ur is the oldest known Archean supercontinent, having formed 3.0 Ga ago by joining the Indian subcontinent's Dharwar and Singbhum cratons, South Africa's Kaapvaal craton, and Western Australia's Pilbara cratons (Rogers and Santosh, 2003) (Fig. 9.6). According to Rogers and Santosh (2003), the Yilgarn and Zimbabwe cratons accreted with the original Ur~2.500 Ga to form the extended Ur. The structure of crustal blocks in expanded Ur is thought to exist until the Mesozoic supercontinent Pangea stabilizes. Saha et al. (2015) found 3400–3500Ma zircon in the BuC and linked it to crust formation events in the Dharwar and Singbhum cratons, which were once part of the Ur supercontinent.

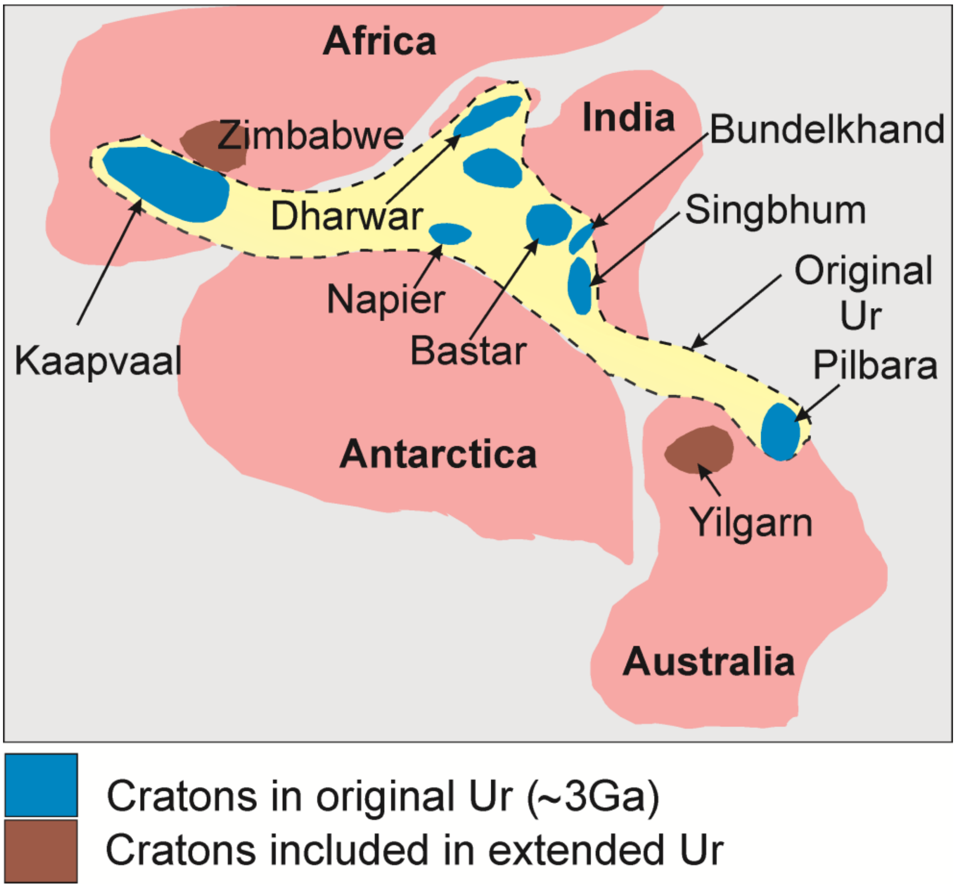


**Figure 9.6** (a) Configuration of extended Ur after Rogers and Santosh (2010).

Raza et al. 2022 reported A2 type granite from the Bastar craton with an age of 2.470 Ga, claiming that these rocks were deposited as part of the extended Ur supercontinent's amalgamation process.

Williams et al. (1991) named the Canadian Shield Kenorland and proposed that Kenorland became a continent at ~2.500 ga but then drifted apart into at least three separate regions. Slabunov and Singh 2020 studied the crustal evolution of Dharwar, Arawali and Bundelkhand Craton and argued them as a part of the Kenorland supercontinent. The 3.6–3.2 Ga TTGs and the 3.43 Ga mafic-ultramafic complexes were reported in the central BuC. Similarly, 3.3–3.2 Ga TTG gneisses from Aravalli Craton and 3.36–3.2 Ga TTGs from the Western Dharwar Craton were also reported. Crustal development in the BuC is comparable to that of the Eastern Dharwar Craton in terms of time and geodynamic pattern, but several key distinctions exist. Subduction occurred in an island-arc regime in the Eastern Dharwar Craton and an active continent margin regime in the BuC. The Western and Eastern Dharwar Cratons were involved as one structure in an accretion-collision event in the late Neoarchean (ca. 2.5 Ga), giving rise to southern Dharwar Craton granulites. Thus, comparing the crustal history of the Bundelkhand, Aravalli, Western, and Eastern Dharwar Cratons demonstrates that geodynamic mechanisms similar to present plate-tectonic and mantle-plume mechanisms were operating during that time. Based on the age data and geodynamic settings of the Archean rocks reported from these cratons, it seems that the Bundelkhand, the Aravalli, and the Western and Eastern Dharwar Cratons appear to have been portions of the Kenorland Supercontinent in Archean times. The Kenorland Supercontinent (Fig. 9.7) is crescentic form according to the paleotectonic reconstruction based on geological and paleomagnetic data (Lubnina and Slabunov, 2009, 2011, 2017; Slabunov and Lubnina, 2016). In the Meso-Neoarchean period (2.9–2.7 Ga), subduction-accretion processes gave birth to the active expansion of the continental crust in the northern portion of the Kenorland supercontinent, whilst plume processes and subduction processes prevailed in the southern section (Lubnina and Slabunov, 2011).

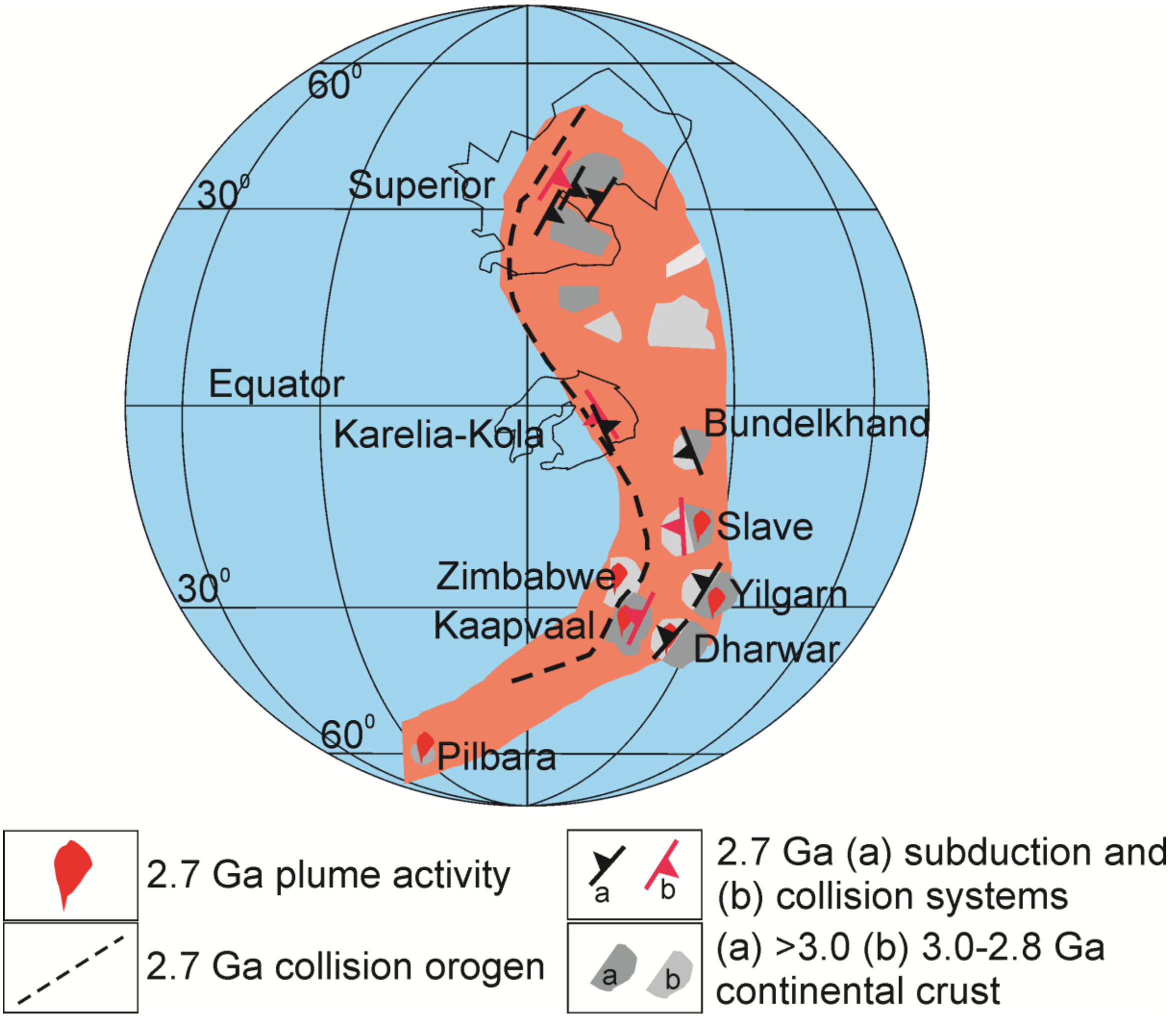


**Figure 9.7** A reconstruction of the Kenorland supercontinent in the Neoarchean (ca. 2.7 Ga) and the Bundelkhand, Dharwar and Aravalli Cratons locations (after Slabunov and Singh, 2018).

This evidence supported that the Mesoarchean subduction-accretion processes in the BuC were similar to those of the Karelian Craton and the Superior Province in the northern half of the Kenorland supercontinent. In the Neoarchean (ca. 2.6 Ga), the core of the supercontinent was formed, and until then, the crust of the southern part of the supercontinent continued to grow during subduction and accretion processes in the Bundelkhand, Aravalli and Western and Eastern Dharwar Cratons (Fig. 9.7).